Azapentacene

International Edition: DOI: 10.1002/anie.201603177
German Edition: DOI: 10.1002/ange.201603177

The Radical Anion and Dianion of Tetraazapentacene

Lei Ji, Martin Haehnel, Ivo Krummenacher, Philipp Biegger, Florian L. Geyer, Olena Tverskoy, Manuel Schaffroth, Jie Han, Andreas Dreuw, Todd B. Marder, and Uwe H. F. Bunz**

Dedicated to Professor Klaus Müllen

Abstract: *The mono- and bis-reduction of 6,13-bis((triisopropylsilyl)ethynyl)quinoxalino[2,3-b]phenazine (**1**) with potassium anthracenide in THF is reported. Both the radical anion $\mathbf{1}^{\bullet-}$ and the dianion $\mathbf{1}^{2-}$ were isolated and characterized by optical and structural (single-crystal X-ray diffraction) methods. Solutions of the radical anion $\mathbf{1}^{\bullet-}$ were stable in air for several hours and characterized by EPR spectroscopy. Dianion $\mathbf{1}^{2-}$ is highly fluorescent and photostable.*

Bis(triisopropylsilylethynyl)pentacene (TIPS-pen) (Scheme 1) and its heteroaromatic congeners,[1] including the doubly alkynylated tetraazapentacene (TAP, **1**),[2] are important semiconducting organic molecules.[3] TIPS-pen is a potent p-channel transporter, that is, the charge transport occurs via hopping of holes, produced by the oxidation of its electron-rich aromatic core. TAP, on the other hand, is an n-channel transport material. At the electrode interface in a thin film transistor, TAP is reduced to its radical anion $\mathbf{1}^{\bullet-}$ and the injected electrons then "hop" through adjacent molecules; this process is responsible for charge transport in this material. An important and not easily answered question is whether there is charge pinning in TAP, particularly at the semiconductor–source interface, and potentially also in the thin film semiconductor itself.[4]

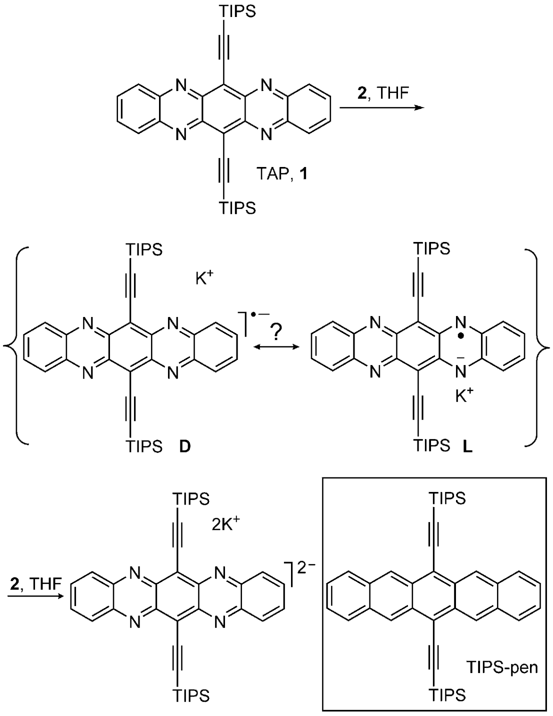

Scheme 1. Reduction of **1** using [K(18-crown-6)(THF)$_2$] anthracenide (**2**) in THF.

In this context, charge pinning would entail that the electron density of the formed radical anions is localized on one or two of the nitrogen atoms—a reasonable assumption on first glance. Does the charge reside at a specific locus of $\mathbf{1}^{\bullet-}$ (the nitrogen atoms, form **L**) or is the charge delocalized over the whole π-system (form **D**)?[2c] This question is fairly difficult to answer when one looks at working devices, for example, transistors containing **1**, because, even if charge pinning would occur, the charge transfer between two adjacent TAP molecules could be degenerate or possibly without a significant activation barrier. Perhaps, more importantly, charge pinning could occur at the interface between the metal and **1** during injection of electrons. In the absence of charge pinning one would assume the charge transfer to have a lower activation barrier. Besides the question of charge pinning, the molecular and electronic structures of the radical anion and the dianion of compounds such as **1** are completely unknown. Thus, investigating their preparation, spectroscopic properties, stability, and structure would not only be of great fundamental interest, but is also important due to the eminent role of **1** in charge transport in n-channel transistors.

In a first experiment, we treated a solution of **1** in THF with [K(18-crown-6)(THF)$_2$] anthracenide (**2**). With one equivalent of **2**, we obtained a dark green-colored solution. Upon slow diffusion of dry *n*-pentane into the reaction mixture, dark crystals formed, which further characterization showed to be the monoanion salt $[\mathrm{K(18\text{-}crown\text{-}6)(THF)_2}]^{+}\mathbf{1}^{\bullet-}$.

---

[*] Dr. L. Ji, Dr. M. Haehnel, Dr. I. Krummenacher, Prof. Dr. T. B. Marder
Institut für Anorganische Chemie
Julius-Maximilians-Universität Würzburg
Am Hubland, 97074 Würzburg (Germany)
E-mail: todd.marder@uni-wuerzburg.de

Dr. P. Biegger, F. L. Geyer, O. Tverskoy, Dr. M. Schaffroth,
Prof. Dr. U. H. F. Bunz
Organisch-Chemisches Institut
Ruprecht-Karls-Universität Heidelberg
Im Neuenheimer Feld 270, 69120 Heidelberg (Germany)
E-mail: uwe.bunz@oci.uni-heidelberg.de

J. Han, Prof. Dr. A. Dreuw
Interdisziplinäres Zentrum für Wissenschaftliches Rechnen
Ruprecht-Karls-Universität Heidelberg
Im Neuenheimer Feld 205, 69120 Heidelberg (Germany)

Supporting information for this article can be found under:
http://dx.doi.org/10.1002/anie.201603177.

Upon addition of two equivalents of **2**, the color of the solution changed dramatically to red. Again, by slow diffusion of dry *n*-pentane into the reaction mixture, $[K(18\text{-crown-}6)THF]^+_2\mathbf{1}^{2-}$ was isolated as dark red crystals. Figure 1 shows the UV/Vis spectra of solutions of the isolated crystals of the monoanion and dianion salts in diethyl ether. Starting with TAP ($\lambda_{max} = 675$ nm), the first reduction leads to a radical anion with a $\lambda_{max} \approx 1400$ nm, i.e., a fairly strong absorption in the near IR. A kinetic scan of the absorption at $\lambda = 792$ nm reveals that the monoanion is stable in dilute THF solution in air for several hours. Upon further reduction, a dramatic blue-shift of the absorption maximum is observed; the dianion produced absorbs at $\lambda_{max} = 592$ nm. A small feature around 792 nm is due to contamination of the dianion with a small amount of the monoanion.

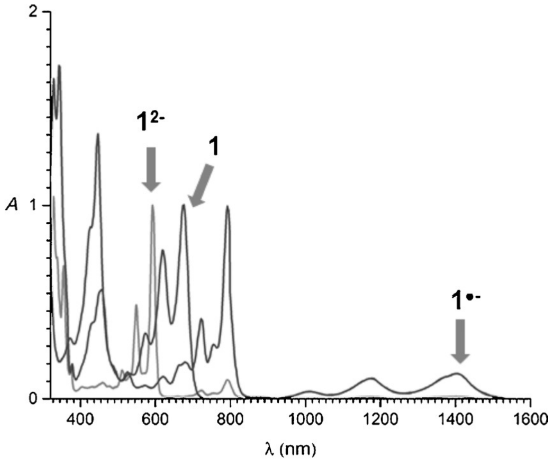

Figure 1. UV/Vis spectra of TAP (**1**) and its monoanion $\mathbf{1}^{\cdot-}$ and dianion $\mathbf{1}^{2-}$ in Et_2O.

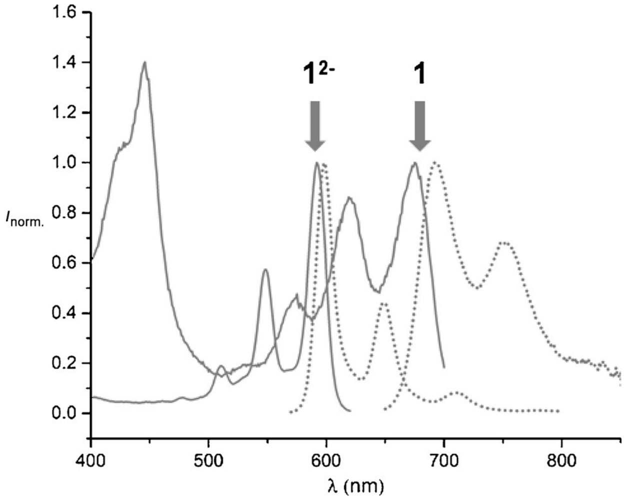

Figure 2. The excitation (solid) and emission (dotted) spectra of $\mathbf{1}^{\cdot-}$ and $\mathbf{1}^{2-}$ in dilute Et_2O.

The dianion, in Et_2O solution, is strongly emissive in the red ($\lambda_{em} = 598$ nm). The excitation spectrum overlaps with the absorption spectrum. Both the absorption/excitation and emission (Figure 2) of the dianion are blue-shifted from that of neutral **1**. The dianion has a higher fluorescence quantum yield (95% vs. 36%) and shorter emission lifetime (6.1 ns vs. 13 ns) than **1**. The Stokes shift of $\mathbf{1}^{2-}$ is small ($\tilde{\nu} = 169\ \text{cm}^{-1}$), indicating that the S_0–S_1 transition is a π–π* transition. Time-dependent (TD) DFT CAM-B3LYP/6-311++G** gas-phase calculations confirmed the S_0–S_1 transitions of **1** (short-axis polarization) and $\mathbf{1}^{2-}$ (long-axis polarization) to be π–π* transitions. The experimentally observed peak of **1** at $\lambda_{max} = 675$ nm corresponds to a pure HOMO–LUMO transition with a calculated excitation energy of 2.01 eV and an oscillator strength of 0.26. The experimental peak of $\mathbf{1}^{2-}$ at $\lambda_{max} = 592$ nm corresponds to the transition from the former LUMO to the former LUMO+1 of the neutral and has an excitation energy of 2.63 eV and an oscillator strength of 0.84 at the theoretical level of TDDFT/CAM-B3LYP/6-311++G** (see the Supporting Information for more details). The near-IR absorption of $\mathbf{1}^{\cdot-}$ originates from an excitation of an electron from the former HOMO to the former LUMO of **1**, which is now singly occupied in $\mathbf{1}^{\cdot-}$. The corresponding state is thus also a π–π* transition with a computed excitation energy of 1.06 eV. Due to the open-shell nature of $\mathbf{1}^{\cdot-}$, its electronic states are not easily interpretable in the molecular orbital picture. In dilute solution, $\mathbf{1}^{2-}$ is photostable. The absorption and emission spectra of a dilute Et_2O solution of $\mathbf{1}^{2-}$, which has been stored in the glove box for more than one month under natural light, are unchanged.

The EPR spectrum (Figure 3) of the radical anion $\mathbf{1}^{\cdot-}$ exhibits a detailed structure composed of hyperfine lines corresponding to the interaction of the unpaired electron with the azaacene ring ($a(^{14}N) = 1.9$ G, $a(^1H) = 0.55$ and 0.50 G) and the silyl groups ($a(^1H) = 0.48$ G (methine protons)), suggesting that the unpaired spin density is not confined to the azaacene unit, but also spills over to the silyl substituents.[5] As a result of the more extended π-system, the observed nitrogen coupling constant is reduced compared to the value for the radical anion of 1,4,5,8-tetraazaanthracene

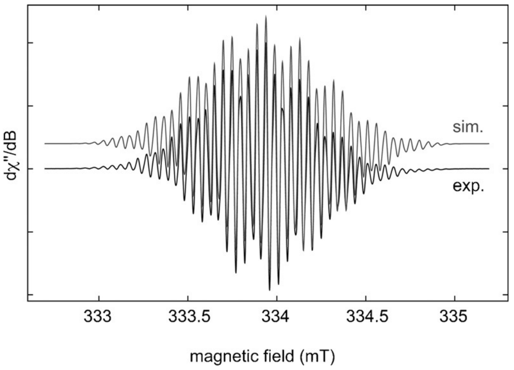

Figure 3. Experimental (black) and simulated (gray) continuous-wave (CW) X-band EPR spectra of $\mathbf{1}^{\cdot-}$ in a toluene/THF mixture at room temperature. Experimental parameters: temperature = 298 K; microwave frequency = 9.38 GHz; microwave power = 0.1 mW; modulation amplitude = 0.1 G; conversion time = 120 ms; modulation frequency = 100 kHz.

($a(^{14}N) = 2.4$ G).[6] We conclude, therefore, that, with regard to EPR, $\mathbf{1}^{\bullet-}$ is delocalized. DFT calculations (Figure 4) also show the absence of any charge pinning in the radical anion, as the electrostatic potential map of $\mathbf{1}^{\bullet-}$ demonstrates that the charge is distributed over the whole π-system. This is also the case for dianion $\mathbf{1}^{2-}$ in the absence of counterions.

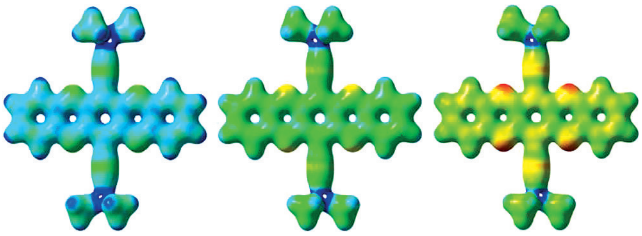

Figure 4. Electrostatic potential (DFT, all same range and iso value). Blue: positive value, red: negative electrostatic potential. Left: Neutral TAP, middle: radical anion, right: dianion.

The molecular structures of $\mathbf{1}^{\bullet-}$ and $\mathbf{1}^{2-}$ are depicted in Figure 5. Both compounds crystallize as centrosymmetric molecules sitting on inversion centers. The important bond lengths of the tetraazapentacene cores are summarized in Figure 6. In $\mathbf{1}^{\bullet-}$, the K^+ ion is fully separated from the heteroacene; it is coordinated by two THF molecules and the 18-crown-6 belt around its equatorial coordination sites. So, the K^+ ion does not interact at all with the aromatic unit, giving testament to the absence of charge pinning in $\mathbf{1}^{\bullet-}$. In the case of the dianion, the two potassium ions are not fully screened from the aromatic face, yet inspection of the crystal structure of $\mathbf{1}^{2-}$ shows that the weak coordination of the potassium ion does not seem to influence the bond lengths significantly. The K1–C5 (3.240(2) Å) and K1–C6 (3.264-(2) Å) bond lengths are fairly similar. Notably, the potassium ions do not interact with the pyrazinic nitrogen atoms at all, which is, at first glance, surprising, but upon inspection of the electrostatic potential map (Figure 4), perhaps more understandable.

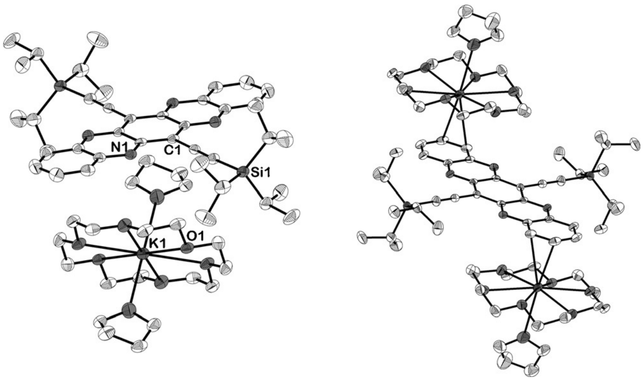

Figure 5. Molecular structure of $\mathbf{1}^{\bullet-}$(left) and $\mathbf{1}^{2-}$ (right) in the solid state. Hydrogen atoms and solvent molecules (THF) in $\mathbf{1}^{\bullet-}$ are omitted for clarity. Atomic displacement parameters correspond to 50% probability at 100 K.

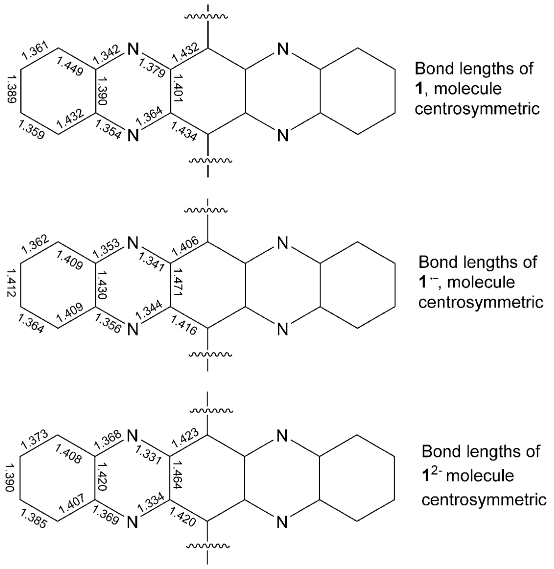

Figure 6. Comparison of the bond lengths obtained from crystal data of **1**, $\mathbf{1}^{\bullet-}$, and $\mathbf{1}^{2-}$. The moderate change of different bond lengths is visible; however, the sum of all unique bond lengths is 1.81 nm for **1**, its radical anion, and its dianion.

In conclusion, we have reduced TAP **1** and obtained both its radical anion $\mathbf{1}^{\bullet-}$ and also its dianion $\mathbf{1}^{2-}$. Both species were investigated by UV/Vis and EPR spectroscopy as well by single-crystal X-ray diffraction analysis. The dianion is a singlet, while $\mathbf{1}^{\bullet-}$ is present as a radical. The reduction does not increase the sum of the bond lengths in the aromatic nucleus but does change some of the bond lengths. From the structural data of $\mathbf{1}^{\bullet-}$, there is no discernible interaction between the potassium ion and the aromatic nucleus in the solid state. As a consequence, there is no detectable charge pinning in TAP $\mathbf{1}^{\bullet-}$, even though the potassium cation is present. The reason for the lack of charge pinning is probably the size of TAP, which allows the negative charge to be easily distributed over the whole molecule. That is perhaps not too surprising as, if one looks at the LUMO, its coefficients are equally distributed over the whole of the molecule. So, the larger the molecule, we posit, the less of an issue charge pinning is, even though electronegative atoms are present in the molecular framework as in **1**.

Experimental Section

All experiments were conducted in an argon-filled glove box. THF was dried by passage through alumina using an SPS system. *n*-Pentane was distilled over $LiAlH_4$ under argon. Diethyl ether was dried by passage through alumina using an SPS system, and stored over NaK in an argon-filled glove-box. [K(18-crown-6)(THF)$_2$] anthracenide was prepared as reported previously.[7]

Preparation of [K(18-crown-6)(THF)$_2$]$^+$$\mathbf{1}^{\bullet-}$: Compound **1** (25 mg, 39 μmol) and [K(18-crown-6)(THF)$_2$] anthracenide (21.5 mg, 35 μmol) were dissolved in 8 mL of dry THF in a 20 mL vial and stirred for 10 min to generate a dark green solution. Dark crystals were formed by slow diffusion of dry *n*-pentane into the reaction mixture. The crystals formed in one week at −30 °C.

Preparation of [K·18-crown-6·THF]$^+_2$$\mathbf{1}^{2-}$: Compound **1** (27 mg, 42 μmol) and [K(18-crown-6)(THF)$_2$] anthracenide (55 mg, 88 μmol) were dissolved in 8 mL of dry THF in a 20 mL vial and stirred for 10 min to generate a dark red solution. Dark red crystals were formed by slow diffusion of dry *n*-pentane into the reaction mixture. The crystals formed in one week at −30 °C.

EPR measurements at X-band (9.38 GHz) were carried out at room temperature using a Bruker ELEXSYS E580 CW EPR spectrometer. CW EPR spectra were measured using 0.1 mW microwave power and 0.1 G field modulation at 100 kHz, with a conversion time of 120 ms. The spectral simulations were performed using MATLAB 8.6 and the EasySpin 5.0.18 toolbox.[8]

UV/Vis-NIR absorption spectra were measured on a Varian Cary 5E UV/Vis-NIR spectrophotometer or on an Agilent 8453 diode-array UV/Vis spectrophotometer. The emission and excitation spectra were recorded using an Edinburgh Instruments FLSP920 spectrometer equipped with a double monochromator for both excitation and emission, operating in right angle geometry mode. All solutions used in photophysical measurements had concentrations of ca. 10^{-5} M in Et_2O, except where stated. The fluorescence quantum yields were measured using a calibrated integrating sphere (150 mm inner diameter). All absorption and emission spectra were recorded in standard quartz cuvettes (1 cm × 1 cm) under argon.

Acknowledgements

We thank the Deutsche Forschungsgemeinschaft (DFG Bu771/7-2) and the Universität Würzburg for support.

Keywords: azapentacene · charge pinning · EPR spectroscopy · radical anions

How to cite: *Angew. Chem. Int. Ed.* **2016**, *55*, 10498–10501
Angew. Chem. **2016**, *128*, 10654–10657

[1] a) J. E. Anthony, J. S. Brooks, D. L. Eaton, S. R. Parkin, *J. Am. Chem. Soc.* **2001**, *123*, 9482–9483; b) M. M. Payne, S. R. Parkin, J. E. Anthony, C. C. Kuo, T. N. Jackson, *J. Am. Chem. Soc.* **2005**, *127*, 4986–4987; c) J. E. Anthony, *Chem. Rev.* **2006**, *106*, 5028–5048; d) J. E. Anthony, *Angew. Chem. Int. Ed.* **2008**, *47*, 452–483; *Angew. Chem.* **2008**, *120*, 460–492; e) J. E. Anthony, D. L. Eaton, S. R. Parkin, *Org. Lett.* **2002**, *4*, 15–18; f) S. Guo, S. K. Mohapatra, A. Romanov, T. V. Timofeeva, K. I. Hardcastle, K. Yesudas, C. Risko, J. L. Bredas, S. R. Marder, S. Barlow, *Chem. Eur. J.* **2012**, *18*, 14760–14772; g) N. L. Holy, *Chem. Rev.* **1974**, *74*, 243–277; h) D. B. Xia, X. Guo, L. Chen, M. Baumgarten, A. Keerthi, K. Müllen, *Angew. Chem. Int. Ed.* **2016**, *55*, 941–944; *Angew. Chem.* **2016**, *128*, 953–956.

[2] a) S. Miao, A. L. Appleton, N. Berger, S. Barlow, S. R. Marder, K. I. Hardcastle, U. H. F. Bunz, *Chem. Eur. J.* **2009**, *15*, 4990–4993; b) Z. X. Liang, Q. Tang, J. B. Xu, Q. A. Miao, *Adv. Mater.* **2011**, *23*, 1535–1539; c) Z. X. Liang, Q. Tang, R. X. Mao, D. Q. Liu, J. B. Xu, Q. Miao, *Adv. Mater.* **2011**, *23*, 5514–5517.

[3] a) U. H. F. Bunz, J. U. Engelhart, *Chem. Eur. J.* **2016**, *22*, 4680–4689; b) U. H. F. Bunz, *Acc. Chem. Res.* **2015**, *48*, 1676–1686; c) U. H. F. Bunz, J. U. Engelhart, B. D. Lindner, M. Schaffroth, *Angew. Chem. Int. Ed.* **2013**, *52*, 3810–3821; *Angew. Chem.* **2013**, *125*, 3898–3910; d) U. H. F. Bunz, *Pure Appl. Chem.* **2010**, *82*, 953–968; e) U. H. F. Bunz, *Chem. Eur. J.* **2009**, *15*, 6780–6789; f) Q. Miao, *Synlett* **2012**, 326–336; g) G. J. Richards, J. P. Hill, T. Mori, K. Ariga, *Org. Biomol. Chem.* **2011**, *9*, 5005–5017; h) J. Li, Q. Zhang, *ACS Appl. Mater. Interfaces* **2015**, *7*, 28049–28062.

[4] a) H. Peisert, A. Petr, L. Dunsch, T. Chasse, M. Knupfer, *ChemPhysChem* **2007**, *8*, 386–390; b) C. Tengstedt, W. Osikowicz, W. R. Salaneck, I. D. Parker, C. H. Hsu, M. Fahlman, *Appl. Phys. Lett.* **2006**, *88*, 053502; c) M. Fahlman, A. Crispin, X. Crispin, S. K. M. Henze, M. P. de Jong, W. Osikowicz, C. Tengstedt, W. R. Salaneck, *J. Phys. Condens. Matter* **2007**, *19*, 183202.

[5] The best possible simulation with couplings to only the nitrogen and hydrogen atoms of the azaacene unit produces a root-mean-square deviation from the experimental spectrum that is almost twice as large.

[6] a) A. Carrington, J. dos Santos-Veiga, *Mol. Phys.* **1962**, *5*, 21; b) F. Gerson, W. Huber, *Electron Spin Resonance Spectroscopy of Organic Radicals*, Wiley-VCH, Weinheim, **2003**.

[7] S. V. Rosokha, J. K. Kochi, *J. Org. Chem.* **2006**, *71*, 9357–9365.

[8] S. Stoll, A. Schweiger, *J. Magn. Reson.* **2006**, *178*, 42–55.

Received: March 31, 2016